

THE EFFECT OF PARTICLE SIZE AND COMPOSITION ON THE PERFORMANCE OF THE COMPOSITE PARTICLE MODEL IN PREDICTING COMBUSTION BEHAVIOUR IN A FLASH FURNACE REACTION SHAFT

Christopher B. SOLNORDAL¹, Frank R.A. JORGENSEN² and Robin RUSSELL³

¹ CSIRO Minerals, Clayton, Victoria 3169, AUSTRALIA

² formerly with CSIRO Minerals, Clayton, Victoria 3169, AUSTRALIA

³ BHP-Billiton Olympic Dam – Smelter, Roxby Downs, South Australia 5725, AUSTRALIA

ABSTRACT

CFD modelling has been used for many years to evaluate the performance of flash furnace burners. Gas flows are modelled using the conventional Eulerian approach, while Lagrangian particle tracking is used to model the flow of solid feed through the burner and into the reaction shaft. The Composite Particle Model (CPM) previously developed by CSIRO, considers the solid feed to be made up of single particles containing concentrate, dust and flux, which then react with surrounding gases using standard heat and mass transfer relationships. However, this approach becomes highly sensitive to the assumed size of the single particle on furnaces that use very fine feed materials, such as BHP-Billiton's Olympic Dam copper flash furnace which was investigated in this work. In this paper the CPM is modified to consider combinations of different particle sizes and compositions. Model performance and stability was significantly improved by modelling the flux as separate large particles in combination with smaller composite particles made up of only concentrate and dust. Further dividing the concentrate/dust particles up into four size fractions increased the computational effort required to achieve a result with very little difference in predicted reaction rate or gas distribution in the reaction shaft. It is concluded that future modelling work for Olympic Dam with the CPM should consider only the concentrate and dust components in the composite particle, with the coarser flux modelled as separate inert particles. This approach has very little computational overhead whilst providing for improved simulation of the reactions in the furnace shaft.

NOMENCLATURE

| | |
|---------------------------------|--|
| D_h | inlet hydraulic diameter |
| g | acceleration due to gravity |
| H | enthalpy |
| $k; k_{in}$ | turbulent kinetic energy; k at inlet |
| p | pressure |
| Q_s | enthalpy source terms |
| T | temperature |
| $\mathbf{u}; \mathbf{u}_{in}$ | velocity vector; \mathbf{u} at inlet |
| $\mathbf{u}'\mathbf{u}'$ | Reynolds stress tensor |
| X_i | mass source term for gas species i |
| Y_i | mass concentration of gas species i |
| $\varepsilon; \varepsilon_{in}$ | turbulence energy dissipation rate; ε at inlet |
| Γ | mass diffusivity |
| λ, μ, ρ | fluid thermal conductivity; viscosity; density |

INTRODUCTION

Detailed mathematical models of the flows and reactions within the reaction shaft of a flash smelting furnace allow deeper understanding of furnace performance, as well as optimization of burner geometry and process conditions. The Composite Particle Model (CPM) is a purpose-built computational model of flash smelting solid feed reactions developed by CSIRO (Koh and Jorgensen, 1994; Koh *et al.*, 1998) and validated against plant measurements (Solnordal *et al.*, 2006b), which runs as part of the commercial CFD package CFX4.4 (AEA Technology, 2001). Up to now Olympic Dam modelling studies have simulated the flash furnace solid feed using mono-sized composite particles containing concentrate, flux and returned dust. The particles are tracked through an Eulerian continuum of gases using a Lagrangian tracking approach. Detailed development history is provided by Solnordal *et al.* (2006a).

Ideally the Lagrangian particle tracking of solid feed into a flash furnace reaction shaft should individually model the billions of particles entering the furnace shaft. This approach is impractical using current technology. Instead a selection of particle paths are calculated, each one representing particles of a given size and composition, entering the flow domain from a specific location with a specific velocity. In previous work (Koh and Jorgensen, 1994; Koh *et al.*, 1998; Solnordal *et al.*, 2006a; Solnordal *et al.*, 2006b) the CPM considered all components of solid feed to be present in each particle. A particle size was then selected that represented the entire range of particle sizes entering the furnace. In this way a large number of tracks could be calculated, giving a statistically valid representation of the solid/gas interactions in the shaft.

Earlier work (Koh and Jorgensen, 1994; Koh *et al.*, 1998) proved the model to be highly robust under the operating conditions of the furnaces studied, due to the relative uniformity in size of the feed. However the feed used in the Olympic Dam smelter is highly non-uniform. Table 1 shows the feed size analysis where the concentrate is very finely ground ($p_{50} < 12 \mu\text{m}$), the recycle dust is four times larger, and the flux over twenty times larger. The representation of the feed stream with a single particle size is therefore less valid than for previous work using more uniform feed blends. Furthermore, the large flux component is assumed inert in the reaction shaft, so its

Table 1. Mineralogical analysis, feed sizing analysis, and oil properties.

| Mineralogical Analysis (wt%) – Cu:S = 1.85; 90% sulphides | | | | |
|---|--|------|------|------|
| Mineral | | Con | Dust | Flux |
| Chalcopyrite | CuFeS ₂ | 31.1 | - | - |
| Bornite | Cu ₅ FeS ₄ | 22.5 | - | - |
| Digenite | Cu ₉ S ₅ | 23.0 | - | - |
| Covellite | CuS | 9.9 | - | - |
| Pyrite | FeS ₂ | 3.5 | - | - |
| Hematite | Fe ₂ O ₃ | 3.8 | - | - |
| Sericite | KAl ₃ Si ₃ O ₁₀ (OH) ₂ | 4.0 | - | - |
| Quartz | SiO ₂ | 2.1 | 3.0 | 100 |
| Copper Sulphate | CuSO ₄ | - | 54.5 | - |
| Copper Oxide | CuO | - | 16.3 | - |
| Cupro-spinel | CuO.Fe ₂ O ₃ | - | 26.2 | - |

| Feed Sizing Analysis (µm) | | | Oil Properties | |
|---------------------------|-----|------|----------------|--|
| % passing | Con | Dust | Flux | Blend of waste oil and diesel |
| 50% | 12 | 52 | 280 | Approximated to C ₁₂ H ₂₂ Heat of reaction = -4.57 × 10 ⁷ J/kg C ₁₂ H ₂₂ |
| 75% | 18 | 70 | 330 | |
| 90% | 28 | 100 | 410 | |
| 100% | 40 | 600 | 850 | |

Table 2. Inlet boundary conditions.

| Inlet | Feed | Feed rate | O ₂ (vol%) | Temp (°C) |
|-----------------|---------------------------|-----------------------------|-----------------------|-----------|
| Solids Chute | Concentrate | 70000 kg/hr | - | 40 |
| | Dust | 8400 kg/hr | - | 40 |
| | Flux | 3570 kg/hr | - | 40 |
| Combustion gas | Enriched air | 37976 Nm ³ /hr | 40 | 40 |
| Dispersion jets | Air | 1297 Nm ³ /hr | 21 | 40 |
| Central pipe | Industrial O ₂ | 810 Nm ³ /hr | 95 | 40 |
| Oil burners | Oil | 62.8 kg/hr/bnr | - | 60 |
| | Enriched air | 178 Nm ³ /hr/bnr | 45 | 60 |

inclusion in the composite particle delays the onset of ignition and subsequent reaction. To counteract this effect, the specified composite particle size must be very small (validation work suggests a value of 18 µm, Solnordal *et al.*, 2006b). When tracking particles of this size through a turbulent gas stream, instabilities in the flow field are appreciable and attempted simulations under steady-state conditions become unreliable. However more recent plant sampling showed the comparatively large flux behaved as separate particles whereas the concentrate and dust tended to form aggregates (Jorgensen *et al.*, 2005).

For the reasons outlined in the previous paragraph the CPM was modified in this work to consider simulation under a variety of different particle size compositions and size distributions. This paper presents the results of the model performance using a distribution of particle sizes, as well as performance when modelling flux as separate particles.

THE OLYMPIC DAM COPPER SMELTER

The copper flash smelter at Olympic Dam is one of two smelters that use Outotec's Direct Blister Flash Smelting technology. Figure 1 (a) shows the layout of the reaction shaft and settler (shown as a half-slice). Copper concentrate, together with returned dust, flux and oxygen-enriched air enter the reaction shaft through a central burner. Additional heat is provided by three oil burners

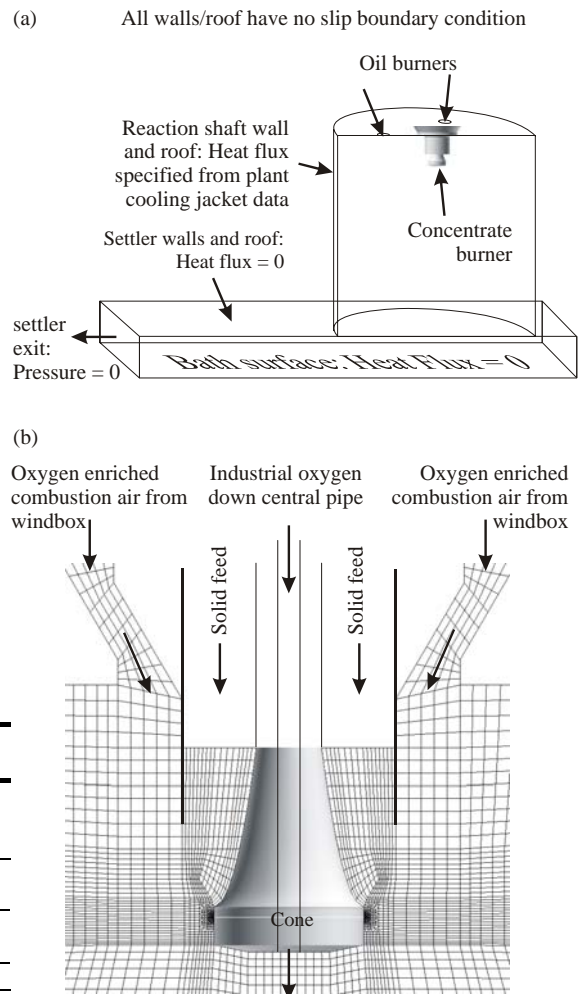


Figure 1: (a) Isometric view of reaction shaft and settler, looking north. (b) Detail of concentrate burner, showing feed inlets and high density mesh around the dispersion cone.

positioned around the concentrate burner. The solids react with oxygen in the reaction shaft; liquid metal and slag separate in the bath and gases and dust exit through the settler. The mineralogical feed composition and size is shown in Table 1.

The concentrate burner is a dispersion burner (Figure 1 (b)). Solid feed passes down a central chute and over a profiled cone. Small air jets positioned around the cone further aid dispersion of the feed. Oxygen-enriched air enters through a wind box, passes through an annular velocity control device and enters the reaction shaft in close proximity to the solids, thus enabling rapid mixing and combustion. Feed rates of all solids, gas and oil are specified in Table 2.

MODEL DESCRIPTION

The original model of the Olympic Dam smelter considered solid feed particles (containing concentrate, flux, dust) and fuel oil droplets tracked using Lagrangian techniques through an Eulerian continuum of gas, with mass and heat being transferred to and from the gas as reactions take place. To calculate the gas flow field, the model solves the Reynolds averaged Navier-Stokes equations for steady-state incompressible flow, together with the energy equation, Equations (1)-(3).

$$\nabla \cdot (\rho \mathbf{u}) = \sum_{i=1,n} X_i \quad (1)$$

$$\nabla \cdot (\rho \mathbf{u} \mathbf{u}) = -\nabla p + \rho g + \nabla \cdot \mu \nabla \mathbf{u} - \nabla \cdot (\rho \overline{u' u'}) \quad (2)$$

$$\nabla \cdot (\rho \mathbf{u} H) = \nabla \cdot \lambda \nabla T - Q_s \quad (3)$$

In Equation (1), $\sum X_i$ is a source term representing the net mass transferred between the particulate and gas phases, where X_i is the source of gas component i , and $X_i > 0$ represents transfer of X_i to the gas. A buoyancy term, ρg , is included in Equation (2). Additional heat is transferred to the gas via radiation (modelled using the technique of Lockwood and Shah, 1980), while heat is also transferred between the gas and particulate phases, and is generated by both gas and solid reactions. These enthalpy source terms are represented by Q_s in Equation (3), where $Q_s > 0$ represents heat transfer from the gas. Turbulence was modelled using the standard $k-\epsilon$ model of Launder and Spalding (1974). Other terms have their usual meanings.

Additional scalar equations (4) are used to calculate the distribution of gas chemical species (namely $C_{12}H_{22}$, O_2 , SO_2 , CO_2 , H_2O) throughout the reaction shaft. In equation (4), Y_i and X_i represent the mass concentration and sources of gas species i , respectively.

$$\nabla \cdot (\rho \mathbf{u} Y_i) = \nabla \cdot \Gamma \nabla Y_i + X_i \quad (4)$$

Both the solid feed and fuel oil were modelled by tracking a small number of individual particles through the continuum fluid. For each particle or droplet Newton's second law is applied, where the force on each particle is made up of drag and buoyancy components (Clift *et al.* 1978). The mass and temperature of the particle varies with position as chemical reactions take place. Heat is transferred between the particle and gas by convection and radiation. Oil droplets were simulated using a total of 60 particle tracks. The number of feed tracks varied as shown in Table 3. Simulation of particle turbulent dispersion was achieved using the stochastic process of Gosman and Ioannides (1981).

Table 3. Particle size/compositions modelled.

| Particle size | Runs 1-3 (con/dust /flux) | Run 4 (con/dust) | Run 5 (con/dust) | Run 6 (con/dust) |
|------------------------------|---------------------------|------------------|------------------|------------------|
| 6 μm | | 30% | | |
| 9 μm | | 20% | 50% | |
| 16 μm | 100% (Run 2) | | | |
| 16.5 μm | | 26% | 26% | |
| 18 μm | 100% (Run 1) | | | 96% |
| 20 μm | 100% (Run 3) | | | |
| 31.5 μm | | 20% | 20% | |
| 280 μm (all flux) | | 4% | 4% | 4% |
| TOTAL TRACKS | 1200 | 3000 | 2400 | 1200 |

Flash Furnace Feed Combustion

The original CPM assumed all solid feed (concentrate, flux and returned dust) entered the flow domain in composite particles. The particles undergo a series of reactions, the speed of which depends on the temperature, composition of the particle, and the composition of the gas surrounding the particle. During passage down the reaction shaft the particles receive heat from the gas and the individual sulphide minerals attain their ignition temperatures and commence combustion (Jorgensen, 2002). The main reactions were identified and grouped as

shown in Table 4, where each group of reactions is assumed to take place at a given temperature: either 400 °C, 670 °C or above 800 °C. Gangue minerals in the concentrate, flux and dust also receive heat and were included in the sub-model as sources of mass contributing to the overall heat capacity of the particles.

The smelting process involves oxidation of sulphur and iron present in the concentrate. During this process the CPM assumes that the particle temperature and the degree of sulphur removal vary as shown in Figure 2. A detailed description of the CPM has been presented by Solnordal *et al.* (2006a), and a summary is provided here.

Table 4. Reactions Modelled During Concentrate and Oil Combustion

| | |
|---|--|
| A | $KAl_3Si_5O_{10}(OH)_2 = KAlSi_3O_8 + Al_2O_3 + H_2O$ $2 CuS = Cu_2S + 0.5 S_2$ $2 CuFeS_2 = Cu_2S + FeS + 0.5 S_2$ $FeS_2 = FeS + 0.5 S_2$ $\Delta H_{R400} = +4.66 \times 10^6 \text{ J/kg S}$ |
| B | $2 Cu_5FeS_4 = 5 Cu_2S + 2 FeS + 0.5 S_2$ $CuSO_4 = CuO + SO_2 + 0.5 O_2$ $\Delta H_{R670} = +8.37 \times 10^6 \text{ J/kg S}$ |
| C | $2 CuO + Cu_2S = 4 Cu + SO_2$ $Cu_2S + O_2 = 2 Cu + SO_2$ $FeS + 1.5 O_2 = FeO + SO_2$ $Fe_2O_3 = 2 FeO + 0.5 O_2$ $\Delta H_{R800} = -5.57 \times 10^6 \text{ J/kg S}$ |
| D | $0.5 S_2 + O_2 = SO_2$ $\Delta H_{SO_2} = -1.13 \times 10^7 \text{ J/kg S}$ |
| E | $C_{12}H_{22} + 17.5 O_2 = 12 CO_2 + 11 H_2O$ $\Delta H_{C_{12}H_{22}} = -4.57 \times 10^7 \text{ J/kg } C_{12}H_{22}$ |

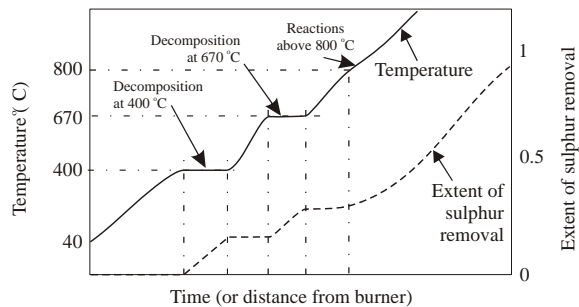


Figure 2: Idealised behaviour of composite particle during combustion.

At temperatures below 400 °C the feed particles heat without reaction. At 400 °C initial reactions occur (Group A, Table 4), with covellite (CuS), chalcopyrite (CuFeS₂) and pyrite (FeS₂) decomposing and liberating labile sulphur (S₂) from the particle. Particle temperature remains constant at 400 °C while labile sulphur is transferred to the gas phase and reacts with oxygen to form SO₂, liberating heat to the gas and back to the particle in accordance with Reaction D (Table 4).

On completion of the Group A reactions, the particle heats to 670 °C where the Group B reactions occur, liberating labile sulphur and small amounts of O₂ and SO₂. The particle then continues to heat from 670 °C to 800 °C when chalcocite (Cu₂S) and ferrous sulphide (FeS) in the

particle undergo further reaction with oxygen in accordance with Reaction Group C (Table 4). These reactions are exothermic and produce heat within the particle, some of which is transferred to the gas phase.

Oil Combustion

The fuel oil used at Olympic Dam has an approximate chemical composition $C_{12}H_{22}$, and is modelled as Reaction E in Table 4 using droplets of diameter $80\ \mu\text{m}$. The reaction rate was determined by chemical kinetics in conjunction with the eddy-breakup combustion model.

Numerical Scheme

CFX4.4 was used to solve equations (1) – (4) using the finite volume method on a co-located body fitted hexahedral grid and the interpolation procedure of Rhie and Chow (1983). Coupling between pressure and velocity was achieved using the SIMPLEC algorithm, a modified form of the SIMPLE algorithm described elsewhere (AEA Technology, 2001; Patanker, 1983). Gas density was modelled assuming it is a function of temperature and gas composition only (AEA Technology, 2001).

Flow Domain, Boundaries and Mesh

The geometry was modelled as a half-slice (Figure 1 (a)). Concentrate and oil entered through Dirichlet inlets, with conditions given in Table 2. Turbulence quantities were estimated at the inlets using empirical functions (Equations (5), AEA Technology, 2001).

$$k_{in} = 0.002 V^2; \quad \epsilon_{in} = k_{in}^{1.5} / (0.3D_h) \quad (5)$$

All solid surfaces, together with the bath surface, were modelled as no-slip wall boundaries. The shaft roof and walls had a constant heat flux distribution determined on-plant to vary between 8 and $56\ \text{kW/m}^2$ out of the flow domain. Other surfaces were assumed to have zero heat flux. The outflow through the settler was modelled as a constant pressure boundary surface.

The body-fitted mesh consisted of approximately 140 000 hexahedral elements. Higher concentrations of cells were used around the concentrate burner, particularly in the region of the disperser jets (Figure 1 (b)), while cell density decreased down the reaction shaft and radially out from the shaft centreline.

Convergence Techniques

Initially an isothermal solution to the gas phase flow field was obtained, and then combusting oil droplets were injected. Composite concentrate particles were then added to the simulation, with their mass flow rate gradually increased to the required mass flow rate of the run. This approach to a stable solution took up to five days, with a total CPU time of approximately 120-160 hours using a single 3.2 GHz PC running Linux. Once a stable solution existed, a new solution using a different composite particle set-up could be achieved in approximately 60 hours.

RESULTS

The conditions of the modelling runs are presented in Table 2, which correspond with typical operating conditions of the plant at the time of the work. Using these conditions, the particle size and composition were changed as shown in Table 3. Initially the solid feed (concentrate, flux and dust) was specified to enter the flow domain as particles of uniform size and composition. The

initial constant particle size of $18\ \mu\text{m}$ (Run 1) was determined by plant validation (Solnordal *et al.*, 2006b). The overall flow pattern of gas in the reaction shaft is shown in Figure 3 in the longitudinal slice through the shaft and settler. Gas passes down the centre of the shaft beneath the concentrate burner. Some gas is predicted to flow straight into the settler, although gas opposite the settler recirculates back into the reaction shaft (red arrows, Figure 3). This flow pattern does not change appreciably in subsequent runs. Instead the effect of changing solid composition is demonstrated using two different plots: a gas temperature distribution in the same vertical plane as the vector plot in Figure 3, and also a graph showing the overall degree of sulphur removal from the solid particles as a function of distance above the settler bath. The temperature plot shows the regions where reaction occurs, while the sulphur removal graph indicates the overall degree of reaction taking place in the reaction shaft.

The temperature distribution for Run 1 (Figure 4 (b)) shows a central plume where the solid feed falls and ultimately ignites and reacts with the surrounding gas. It has been shown from plant measurements (Solnordal *et al.* 2006b) that this cooler plume exists, although it is unlikely to be as cool as predicted in Figure 4. Its true extent into the reaction shaft is unknown.

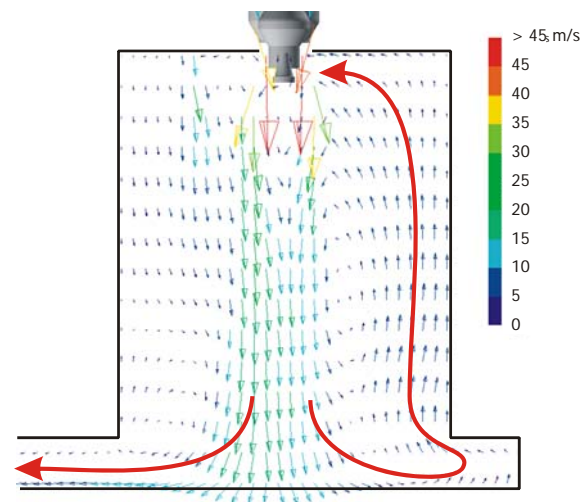


Figure 3: Velocity vector distributions in symmetry plane for Run 1: $18\ \mu\text{m}$ particles.

Sensitivity to Assumed Composite Particle Size

The predicted extent of the plume is greatly affected by the assumed size of the composite particle (Runs 2 and 3, Figure 4 (a) and (c)). Reducing the particle size below $16\ \mu\text{m}$ leads to instabilities in the predicted flow field. The extent of sulphur removal, and hence the degree of solids reaction, also varies significantly for Runs 1-3 (Figure 5).

Sensitivity to Distribution of Particle Sizes

All solid feed was combined into a single composite particle primarily to allow the smallest number of particle tracks to be modelled. To determine the effect of this approach on the solution, in Run 4 the solid feed was

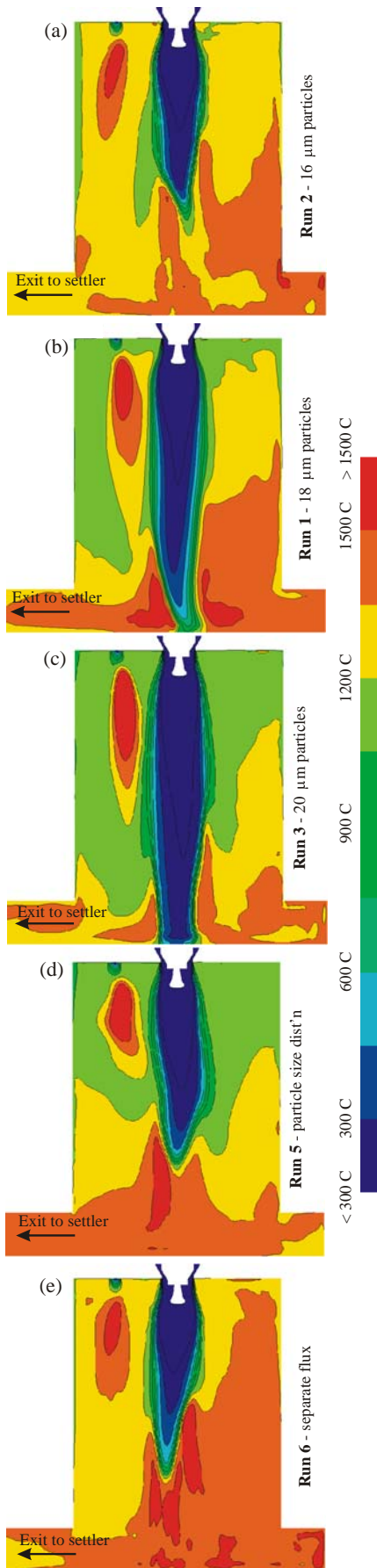


Figure 4. Gas temperature distributions in symmetry plane, Runs 1, 2, 3, 5 and 6.

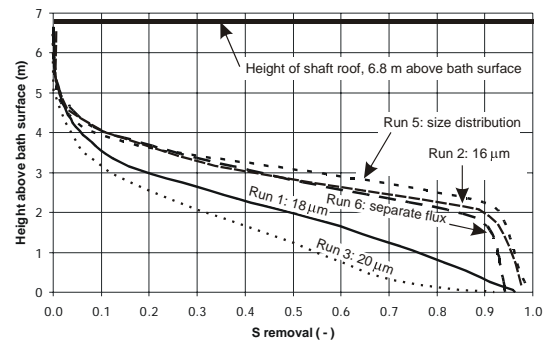


Figure 5. Degree of sulphur removal, as a function of distance from the settler roof. Runs 1, 2, 3, 5 and 6.

instead divided into five different size fractions. The smallest four of these fractions corresponded approximately to the wet size distribution of the concentrate, and feed of this size was assumed to only contain the reactive concentrate and recycle dust. The fifth, and largest, size fraction represented the flux component of the feed, at an average size of 280 μm .

Attempts to run the model with this size distribution failed, as the solids plume was predicted to sway haphazardly around the reaction shaft. It was assumed that the smallest size fraction of 6 μm was causing this effect, as previous work had revealed similar instabilities in the flow field when using small particles. Thus the two smallest size fractions were combined to a single fraction of size 9 μm (Run 5, Table 3) and the model re-run.

The temperature distribution predicted using the size distribution for Run 5 is shown in Figure 4 (d). The length of the plume is similar to that using a mono-sized distribution with particle size of 16 μm (Run 2, Figure 4 (a)). The elimination of sulphur as a function of distance from the bath surface for Run 5 is shown in Figure 5 and is similar to that of Run 2, although sulphur elimination occurs slightly higher in the shaft for Run 5.

A simpler size distribution was then investigated in Run 6. In this case the solids feed was modelled using two size fractions: all of the concentrate and dust was modelled using particles of a single size of 18 μm while the flux component was modelled separately using a size fraction of 280 μm . The model produced a stable result with a temperature distribution shown in Figure 4 (e). The degree of sulphur removal for this run is shown in Figure 5, with the rate of removal being slightly slower than for Run 5.

DISCUSSION

Using the original CPM (with concentrate, flux and dust present in a single mono-sized particle) naturally leads to some compromise in predictive power. There is no opportunity for the very small component of the feed to react rapidly, and the overall heat capacity of the feed is increased by the inclusion of the inert flux component in the particle. Conversely, the total number of particle tracks necessary to simulate the gas/solid reactions is relatively small – 1200 tracks (Runs 1-3) for a 3D half-slice model. When using a particle size distribution (Run 5) the total number of tracks was increased to 3000 so that each particle size was represented throughout the reaction shaft, and this significantly increased the run time for the model.

By introducing a particle size distribution in Runs 4 and 5 it was thought that the point of onset of particle reaction would be spread out over the height of the reaction shaft, but this was not the case. The results in Figure 5 show that Run 5 allowed reaction to start higher in the reaction shaft, and to proceed at a greater rate than for Run 1. However, the overall distribution of temperature was surprisingly similar to that using a mono-sized composite particle, albeit with a smaller diameter (i.e. Run 2).

Once of the advantages in using the particle size distribution of Run 5 was that it was possible to simulate particles as small as 9 μm in diameter, which more closely represent the actual size of the concentrate at Olympic Dam. It had previously been found that using a single mono-sized composite particle smaller than 16 μm caused the CPM to become unstable, whereas the use of 9 μm particles in conjunction with larger ones allowed the solution to become stable. However, as shown by Run 4, there was still a problem with model stability of the smallest particle size modelled was reduced to 6 μm .

When comparing Runs 5 and 6 the particle reactions (represented by removal of sulphur) occur higher up the reaction shaft than for Run 1 (Figure 5), and the ongoing reaction rate is similar (although reactions in Run 6 do proceed marginally faster than for Run 5). This result suggests that it is primarily the decoupling of flux from the composite particle that allows the prediction of the reaction to proceed higher up in the shaft and at a faster rate. In Run 6 the reaction shaft is predicted to be hotter than for Run 1, and the integrated gas exit temperature is 1360 $^{\circ}\text{C}$, compared to 1290 $^{\circ}\text{C}$ for Run 1. The final average temperature of the flux particles as they reach the bath surface is 1130 $^{\circ}\text{C}$, compared with 1420 $^{\circ}\text{C}$ for the composite concentrate/dust particles. Thus the flux is still providing a heat sink, but is not inhibiting the heating up and reaction of concentrate and dust to the same extent as for Runs 1-3. Furthermore, by only having two types of particles (instead of four) the approach of Run 6 is more computationally efficient than Run 5.

CONCLUSIONS AND RECOMMENDATIONS

The Composite Particle Model of flash furnace reactions has been used under two new conditions: using a four-component particle size distribution, and using a two-component distribution where inert flux is separated out from the reactive concentrate and dust components of the feed. Both of these methods predicted the gas/solid reactions to commence higher in the shaft compared with the conventional single mono-sized particle containing all three feed components. The gas/solid reactions also proceeded at a greater rate, equivalent to using a single mono-sized particle 10% smaller than recommended by Solnordal *et al.* (2006b) based on plant trials.

It was found that the use of four size fractions in the particle size distribution allowed a marginally faster degree of reaction over the use of only two sizes, suggesting that it is the decoupling of inert flux from reactive concentrate and dust that has the more significant effect on the model performance.

It is recommended that future modelling the Olympic Dam furnace with the Composite Particle Model use the approach of separating out flux from the composite particle. This will allow a more stable solution (as larger

particles can be used to achieve the same degree of reaction in the model) with only a modest increase in computational effort over the single particle approach used previously by the authors.

ACKNOWLEDGEMENTS

The authors wish to acknowledge the assistance in this work of Dr Andrew Campbell, formerly of BHP-Billiton, for his useful input during the modelling campaign.

REFERENCES

- AEA TECHNOLOGY, (2001), CFX-4.4: *Solver Manual*, Harwell Laboratory, Oxfordshire, UK.
- CLIFT, R., GRACE, J.R. and WEBER, M.E., (1978), *Bubbles Drops and Particles*, Academic Press.
- GOSMAN, A.D. and IOANNIDES, E., (1981), "Aspects of computer simulation of liquid fuelled combustors", A.I.A.A. Paper No. 81-0323.
- JORGENSEN, F.R.A., (2002), "The Ignition of Sulphide Flotation Concentrates in Flash Smelting", *Sulphide Smelting 2002*, R. L. Stevens and H. Y Sohn Eds. TMS Warrendale, Pa., 49-60.
- JORGENSEN, F.R.A., CAMPBELL, A., TAYLOR, R. AND WASHINGTON, B. (2005), "Sampling and Measurement in the Reaction Shaft at Olympic Dam", *First Extractive Metallurgy Operators Conference*, Aus IMM, Melbourne, Australia, 87-93.
- KOH, P.T.L. and JORGENSEN, F.R.A., (1994), "Modelling Particulate Flow and Combustion in a Flash Smelter", *CHEMECA '94*, Proceedings of the 22nd Australian Chemical Engineering Conference, Perth, WA, Australia, 499-506.
- KOH, P.T.L., NGUYEN, T.V. and JORGENSEN, F.R.A., (1998), "Numerical Modelling of Combustion in a Zinc Flash Smelter", *Appl. Math. Model.*, **22** (11), 941-948.
- LAUNDER, D.E. and SPALDING, D.B., (1974), "The Numerical Computation of Turbulent Flows", *Comp. Meths. Appl. Mech. Engng*, **3**, 269-289.
- LOCKWOOD, F.C. and SHAH, N.G., (1980), "A New Radiation Solution Method for Incorporation in General Combustion Predictions Procedures," *Proceedings of the 18th Symposium (Int.) on Combustion*, The Combustion Institute, 1405-1414.
- PATANKER, S.V., (1983), *Numerical Heat Transfer and Fluid Flow*, Hemisphere.
- RHIE, C.M. and CHOW, W.L., (1983), "Numerical study of the turbulent flow past an airfoil with trailing edge separation, *AIAA J*, **21**, 1527-1532.
- SOLNORDAL, C.B., JORGENSEN, F.R.A., KOH, P.T.L. and HUNT, A., (2006a), "CFD Modelling of the flow and reactions in the Olympic Dam flash furnace smelter reaction shaft", *Appl. Math. Model.*, **30**, 1310-1325.
- SOLNORDAL, C.B., JORGENSEN, F.R.A., and CAMPBELL, A., (2006b), "Validation of the Olympic Dam flash furnace burner and reaction shaft model – comparison of the model with plant measurements", *Sohn International Symposium Proceedings, Advanced Processing of Metals and Materials Volume 8: International Symposium on Sulfide Smelting 2006*, San Diego, CA, September 2006, TMS, 687-702.